https://doi.org/10.5194/amt-2021-112
Preprint. Discussion started: 12 May 2021

Atmospheric Measurement Techniques
Discussions

Enhanced MOPITT data coverage through cloud detection improvement

Heba S. Marey[1], James R. Drummond[1], Dylan B. A. Jones[1], Helen Worden[2], Merritt N. Deeter[2], John Gille[2], and Debbie Mao[2]

1 University of Toronto, Department of Physics, Atmospheric Science Group, Ontario, Canada, 2 National Center for Atmospheric Research, Boulder, Colorado, USA.

Abstract

The Measurements of Pollution in the Troposphere (MOPITT) satellite instrument has been measuring global tropospheric carbon monoxide (CO) since March 2000, providing the longest nearly continuous record of CO from space. During its long mission the data processing algorithms have been updated to improve the quality of CO retrievals and the sensitivity to the lower troposphere. Currently, MOPITT retrievals are only performed for clear-sky observations or over low clouds for ocean scenes. Compared to all observed radiances, successful retrieval rates are about 30% and 40% between 90°S–90°N and 60°S–60°N, respectively. Spatial seasonal variations show that while MOPITT data coverage in some places reaches 30% in summer, this number can drop to less than 10% in winter due to significantly increased cloud cover. Therefore, we investigate the current MOPITT cloud detection algorithm and consider approaches to increase the data coverage.

The MOPITT CO total column (TC) data were modified by turning off the cloud detection scheme to allow a CO retrieval result regardless of their cloud status. Analyses of the standard CO TC product (cloud filtered) and non-standard product (non-cloud masked) were conducted for selected days. Results showed some coherent structures that were observed frequently in the non-masked CO product that were not present in the standard product and could potentially be actual CO features. A corresponding analysis of Moderate Resolution Imaging Spectroradiometer

https://doi.org/10.5194/amt-2021-112
Preprint. Discussion started: 12 May 2021

Atmospheric Measurement Techniques Discussions

(MODIS) cloud height and cloud mask products along with MOPITT cloud flag descriptors was conducted in order to understand the cloud conditions present for these apparently physical CO features. Results show that a significant number of low cloud CO retrievals were rejected in the standard product. Those missing areas match the coherent patterns that were detected in the non-masked CO product. Many times, these structures were also seen in the Infrared Atmospheric Sounding Interferometer (IASI) CO TC product indicating actual CO plumes.

Multi-angle Imaging SpectroRadiometer (MISR) data on the Terra satellite were also employed for cloud height comparison with MODIS. Comparisons of MODIS and MISR cloud height data indicate remarkable agreement which is encouraging for the possibility of incorporating MODIS cloud height in the MOPITT cloud detection scheme. Statistics of the global assessment of the potential use of MODIS cloud height shows that MOPITT data increases significantly when cloud heights less than 2 km in height are incorporated in the retrievals. However quality indices should be defined and produced to ensure sufficient retrieval quality.

1. Introduction

Carbon monoxide (CO) in the atmosphere has a medium lifetime (weeks to months), which is long enough to track atmospheric physical and chemical processes over a range of spatial scales from space (Jiang et al., 2011, Edwards et al., 2006; Duncan et al., 2007). Hence, satellite measurements of atmospheric CO are useful for studying both transported and local sources of pollution as well as atmospheric chemistry.

The Measurements of Pollution in the Troposphere (MOPITT) satellite instrument provides the longest dataset of CO from space. It has been measuring tropospheric CO using gas filter correlation radiometry (GFCR) since March 2000 (Drummond et al., 1996, Drummond et al., 2010, Deeter et al., 2017), with a footprint of 22 km × 22 km and global coverage every 3 days (Deeter et al., 2003). It is on board the Terra satellite, which is in a sun-synchronous polar orbit at 705 km of altitude and crosses the equator at 10:30 local time (Drummond et al., 1996). Furthermore, it is the only satellite instrument that measures CO in both the thermal infrared (TIR, 4.7 μm) and near infrared (NIR, 2.3 μm). This long-term data record provides a unique opportunity for analyzing interannual variability and long-term trends in the distribution of CO, atmospheric

https://doi.org/10.5194/amt-2021-112
Preprint. Discussion started: 12 May 2021

Atmospheric Measurement Techniques Discussions

transport, and tropospheric chemistry that are associated with human activity and climate change (Worden et al., 2013; Strode et al., 2013, Buchholz et al., 2021).

During MOPITT's long mission, data processing algorithms have been updated considerably to improve the quality of the CO retrievals and their sensitivity to the lower troposphere. However, MOPITT cannot "see" through cloud and this represents a significant obstruction to measurement spatial coverage. The current cloud detection algorithm, using both MOPITT and MODIS information (Warner, et al., 2001), rejects pixels with a significant amount of cloud cover, thereby reducing the number of pixels retrieved. This leads to global maps with gaps in CO data where clouds are present.

Retrieving CO gas in cloudy conditions represents a major challenge. The presence of clouds in the observed scene enhances reflectivity and blocks the atmosphere below the clouds for cloudy scenes compared to cloud-free sky scenes. The albedo and in-cloud absorption effects enhance the sensitivity to trace gases above the clouds, while the shielding effect impacts the vertical sensitivity of the measurement which results in an inaccurate estimation of the trace gas column. Various techniques have been proposed to cope with this problem depending on the spectral range of the measurements. These techniques can be grouped into the following four approaches.

The first approach is the threshold method, where only observations under clear sky conditions or weakly cloud contaminated scenes (determined by using threshold-based algorithms to detect clouds and develop cloud masks) are considered (Ackerman et al., 1998; Deeter, 2003; Warner, et al., 2001). The second approach, referred to as cloud clearing, is to reconstruct clear column radiances that would have been present if there were no clouds. Cloud clearing is used for Atmospheric Infrared Sounder (AIRS) atmospheric CO retrievals where a reconstructed pixel consisting of a 3 x 3 array (9 pixels are used) is produced, resulting in 45 km spatial resolution (Susskind et al., 2003; Li et al., 2005). Both of these approaches avoid the need for complex modeling of cloud effects, but have the added complexity of characterizing errors resulting from un-modeled cloud fields. The third approach is to solve for the radiative effects of clouds directly in the inversion process. This approach is used for retrieving profiles (Kulawik et al. 2006) from measurements from the Tropospheric Emission Spectrometer (TES). The fourth approach is utilized for CO retrievals over land and ocean in the presence of low-altitude clouds from measurements from the TROPOspheric Monitoring Instrument *(*TROPOMI*)*. In this approach, shortwave infrared (SWIR) measurements of methane TC are used to filter out observations with

https://doi.org/10.5194/amt-2021-112
Preprint. Discussion started: 12 May 2021

high and optically thick clouds to retrieve the trace gas information (Vidot et al. 2012, Landgraf et al., 2016).

We considered all four of these approaches for improving MOPITT retrievals under cloudy conditions. However, due to the lack of spectral information and collocated methane data, only the first two approaches are possible and, unfortunately, the results of the reconstructed clear column radiances using two adjacent pixels were not sufficiently precise for viable retrievals. Consequently, adjustments to the current MOPITT cloud detection scheme is the only one of the four approaches that can be employed. The aim of this study is to revisit and improve this scheme in order to increase the coverage of the MOPITT CO dataset.

2. Data and Methodology

This study uses data from three satellite instruments, MOPITT, the Moderate Resolution Imaging Spectroradiometer (MODIS), and the Multi-angle Imaging Spectroradiometer (MISR). MODIS, MISR and MOPITT are all onboard the Terra satellite (crosses the equator at a local time of 10:30 am), which facilitates the collocation of observations in space and time.

2.1 MOPITT

MOPITT Version 7 (V7) Level 1 (L1) and Level 2 (L2) TIR products are used in this study. L1 data corresponds to all of the radiance observations that are obtained in MOPITT swaths. They are used subsequently as input to the algorithms that retrieve the CO vertical profiles and total column (TC) amounts, which are referred to as L2 data. The MOPITT L2 products that are utilized here are the CO total column (TC) abundances, the cloudy MODIS diagnostic, and the flag number (the cloud descriptor). The non-masked L2 product was only available from V7, so V7 is used throughout this paper.

2.2 MODIS

The MODIS products used in this study are the Collection-6 1-km cloud mask (MOD35) and the cloud height 5-km resolution (MOD06) data. MODIS measures radiances at 36 wavelengths, including infrared and visible bands with spatial resolution from 250 m to 1 km. The MODIS cloud mask algorithm uses up to 19 MODIS spectral bands for better cloud detection (Ackerman et al., 2008, 1998). The MODIS cloud height is derived using 5 thermal infrared bands (both day and night) at 5 km spatial resolution.

https://doi.org/10.5194/amt-2021-112
Preprint. Discussion started: 12 May 2021

2.3 MISR

The MISR instrument has a 380 km-wide swath. It provides global coverage every nine days at the equator that repeats precisely every 16 days. It has a unique design for imaging the Earth at nine view angles along the orbit track, ranging from 70° forward, through nadir, to 70 ° aft, in each of four spectral bands centered at 446 nm (blue), 558 nm (green), 672 nm (red), and 866 nm wavelengths. This unique design allows the instrument to retrieve the heights of clouds and aerosol plumes with a horizontal resolution of 275 m. MINX (MISR Interactive Explorer) is a tool for the visualization and analysis of MISR operational stereo products to provide a precise digitization of smoke, volcanic, cloud, or dust plumes at high spatial resolution (Nelson et al. 2009; 2013).

2.4 IASI-A

IASI-A is a Fourier Transform Spectrometer on the European space agency (EPS)/MetOp-A satellite launched in 2006 with a spectral coverage range from 3.62 to 15.5 µm (645 to 2760 cm−1) including the CO 2140 cm^{-1} TIR band. It views the ground through a cross-track rotary scan mirror with a horizontal resolution of 12 km diameter at nadir, which increases at the larger viewing angles. The width of the swath is ~ 2200 km with a total of 120 views. The IASI instrument takes measurements day and night which gives a global coverage twice a day with some gaps between orbits around the equator. However, clouds in the field of view can obstruct the measurements and hence reduce the number of the observations (Clerbaux et al., 2009). This study used L2 IASI-A CO TC values that were retrieved by LATMOS (Laboratoire Atmosphères, Milieux, Observations Spatiales) using a retrieval code, FORLI (Fast Optimal Retrievals on Layers for IASI), developed at ULB (Université Libre de Bruxelles) (https://iasi.aeris-data.fr/co/). Data are retrieved for a cloud fraction of less than 25 % (Clerbaux et al., 2009).

3. MOPITT cloud detection scheme

The MOPITT procedures for identifying clear-sky retrievals from cloud-contaminated pixels involves a threshold method that makes use of two independent tests, (1) a MOPITT radiance ratio threshold and (2) a MODIS cloud mask threshold within the MOPITT field of view (Warner et al., 2001, Deeter, 2011), which are described below.

https://doi.org/10.5194/amt-2021-112
Preprint. Discussion started: 12 May 2021

Atmospheric Measurement Techniques
Discussions

MOPITT radiance threshold. Radiance from the MOPITT 4.7 μm thermal channel radiance is compared to the a priori clear-sky radiance calculated by The MOPITT Operational Fast Forward Model (MOPFAS) for each pixel. If the measured/calculated radiance ratio is ≥1.0 for V8 and ≥ 0.955 for other versions (V7 and before), then the observation is considered "clear". For this test however, the threshold value may be exceeded under temperature inversion conditions where clouds are warmer than the underlying surface. This threshold method is not applicable to polar regions due to the frequent temperature inversions at night, and to avoid the effect of possible snow and ice coverage on the daytime signals (Warner et al., 2001).

The MODIS Cloud threshold. The MODIS swath (2330 km) is much wider than the MOPITT swath (640 km), so it provides complete overlap for MOPITT passes. The MODIS cloud mask (MOD35 L2) product (Ackerman et al., 2008) that is used here has 1 km horizontal resolution at nadir (Ackerman *et al.*, 1998). Therefore, each MOPITT pixel can encompasses ~ 480 MODIS 1 x 1 km pixels. After co-location, relevant MODIS cloud mask parameters of the MODIS are gathered and averaged for each MOPITT pixel. MOD35_L2, containing data collected from the Terra platform is used to get the cloud count at each MOPITT pixel and If the MODIS cloud percent is less than 5%, then the MOPITT pixel is considered clear.

These two threshold tests above are used in conjunction, with the MODIS value superseding the MOPITT value over land, i.e., if MODIS test is "clear" and MOPITT test is "cloudy", then the MOPITT pixel will be considered "clear" (Warner et al., 2001, Marey et al., 2018). However, if the MOPITT test identifies the pixel as clear and the MODIS test identifies the pixel as cloudy, then a low cloud test is done. The low cloud test exploits the MODIS IR and visible reflectance (Warner et al., 2001: Deeter et al., 2017). To assign low clouds for daytime observations, an averaged MODIS IR threshold test value should be ≥0.9 and an averaged MODIS visible reflectance test value should be ≤0.95. For nighttime observations, a MODIS IR temperature difference test value ≥0.9 is interpreted as low clouds (Warner et al., 2001, Marey et al., 2018). While for ocean scenes even if the low cloud test did not pass, the pixel is considered clear based on either the MOPITT or MODIS test result (Deeter et al., 2017).

The final clear/cloudy decision for each MOPITT pixel is based on set of rules summarized in six cloud indices/flags as follows: The pixel is assigned to be clear and hence retrieved if:
1: MODIS data are missing but the MOPITT radiance threshold is passed (rare).
2: MODIS data are clear and the MOPITT radiance threshold is passed. (most confidently clear)

https://doi.org/10.5194/amt-2021-112
Preprint. Discussion started: 12 May 2021

Atmospheric Measurement Techniques Discussions

3: MODIS data are clear but MOPITT radiance threshold is failed. The MODIS result overrides the MOPITT result.

4: MODIS data are cloudy but the MOPITT radiance threshold is passed. In this case, the MODIS low cloud test is applied and in the case of a low cloud, the pixel is treated as clear (occurs mostly over ocean scenes).

5: Polar regions only (> 65° N or S latitude): MODIS data are clear. MOPITT test is not used.

6: Ocean scenes only/no MODIS low cloud: MODIS data are cloudy and the MOPITT radiance threshold is passed. This was introduced in V7 to correct for an observed degradation in MODIS cloud products (Moeller and Frey, 2017).

If the pixel does not pass any of these tests pass, then no retrieval is performed. Table 1 summarizes these tests.

Table 1. MOPITT V7 Cloud Descriptor Values in L2 CO retrievals

Descriptor value	MOPITT assignment	MODIS assignment	Notes
1	clear	missing	MODIS data are not available
2	clear	clear	
3	cloudy	clear	
4	clear	cloudy, low clouds	
5	Not used	clear	Used only in polar regions
6	clear	cloudy, no low clouds	Introduced in MOPITT V7, for ocean observations only

4. Results and Discussion

4.1 Assessment of the current situation

To assess the current MOPITT CO retrieval in terms of data coverage, the statistics of the L2 data from 2000 to 2019 are computed. Buchholz et al. (2017) recommended to avoid the use of MOPITT above 60°N as the sea ice may not be correctly accounted for in the retrievals. The

https://doi.org/10.5194/amt-2021-112
Preprint. Discussion started: 12 May 2021

Atmospheric Measurement Techniques Discussions
Open Access
EGU

fraction of daily valid data between 90°S–90°N and 60°S–60°N are shown in Figure 1. The successful rate is calculated by taking the ratio of the number of daily valid data CO retrievals (L2) to the total number of daily radiance measurements (L1). The successful rate varies between 27%–33% and 34%–42% for the 90°S–90°N and 60°S–60°N domains, respectively, with a clear seasonal effect. Figure 2 shows the spatial coverage rate (the percent of the retrieval number/number of radiance measurements) using 2014 as a representative year (1° × 1° bins). Some regions exhibit high coverage rates (close to 100%) in all seasons, such as northern Africa, whereas other regions exhibit large seasonal variations in terms of data coverage. For example, in Canada, the data coverage reached 50% in summer (e.g. Hudson Bay), but drops to less than 10% in winter due to high cloud cover. In general, high latitude regions (poleward of 65°) have strong seasonal variations in data coverage, with the northern high latitudes showing the highest coverage rates in June, July, and August, and the southern high latitudes exhibiting the highest rates in December, January, and February as a result of less cloud in the summer. Here we focus on daytime data, and therefore there is a cut off at high northern latitudes in the northern-hemisphere winter, and at high southern latitudes in the southern-hemisphere winter. The case studies below are taken over Canada because of high CO variability and the interest in the transport of fire pollution.

4.2 Analysis of standard and non-standard MOPITT product

CO TC were retrieved for a selected number of dates and locations by suppressing the cloud detection scheme, which means that all MOPITT L1 data were used to produce the L2 product regardless of the cloud conditions. This non-cloud masked product will be referred to here as the non-standard product. Analysis of the CO TC V7 L2 standard (cloud filtered) and non-standard product (non-cloud masked) were done for some selected cases. Figures 3a and 3b show the standard and non-standard CO product on 16 August 2018, respectively, over the region between 78°W–92°W and 44°N–60°N, which covers Ontario, Canada, near Hudson Bay. The standard (cloud masked) product indicates that about 60% of the data are missing. Comparing it to the non-standard (non-masked) product, some features can be observed in the non-standard product over the regions that were missing data in the standard product. A coherent structure is present between 50°N–54°N (as it is indicated by pink and purple colors). The IASI TC for the same area and time was analyzed to corroborate whether the features in the non-cloud-masked product are actual CO plumes (Figures 3c). Comparing IASI CO TC on 16 August 2018 (Figures 3c) to the corresponding

https://doi.org/10.5194/amt-2021-112
Preprint. Discussion started: 12 May 2021

MOPITT (Figure 3b) illustrate a strong CO plume around 50-55 latitude and -94: -84 longitudes that is apparent in both IASI and MOPITT. In the next section the MODIS cloud height product was used to diagnose the cause of the missing (not retrieved in the standard product) CO features.

4.3 Regional analysis of MODIS cloud height and MOPITT data

Figures 3d depicts the MOPITT cloud flag description (see Table 1), for the case on 16 August 2018. Retrievals were assigned flag number 2 (MODIS and MOPITT clear, grey color), 3 (MODIS clear and MOPITT cloudy, dark blue), and 4 (low clouds, cyan color). Figures 3d shows that the L2 data on 16 August 2018 case were retrieved based on clear and low cloud conditions as indicated by flag number 2 and flag number 4. Figure 3e displays the MODIS cloud height (and cloud mask for the same swath on 16 August 2018. Comparing the low cloud retrieval area (cyan color) to the corresponding MODIS cloud height (Fig. 3e) and cloud mask (Figure 3f), it can be seen that this area has cloud percent (the term "cloud" encompasses water clouds and aerosols) by more than 90% and has cloud heights less than 1 km, as illustrated by the grey color (Figure 3e). The MODIS cloud height also shows other areas that have low clouds (grey and blue colors) where there were no retrievals in the standard product. Those pixels match with the coherent pattern region (between 52°N–54°N) that were shown in the non-masked product (Figure 3b). Therefore, it appears that some of the potential retrievals are missed in the standard retrieval due to misidentification of low cloud pixels. It is necessary to examine additional cases using the same approach to determine whether these findings are widespread, but it is instructive to first consider an analysis of the cloud heights using MISR data.

4.4 MISR and MODIS height comparison

To assess the reliability of using the MODIS cloud height product, two cloud areas within the field of the same data/time were chosen for cloud height comparison with MISR data. The MISR MINX tool was employed for cloud digitization (cloud height information). The left panel in Figure 4 shows the MODIS cloud height values on 16 August 2016 for the region shown in Figure 3e. Given that the width of the MISR swath is less than that of MOPITT, the yellow box in the figure represents the MISR path that overlaps with MOPITT. The true MISR stripe is presented

https://doi.org/10.5194/amt-2021-112
Preprint. Discussion started: 12 May 2021

in the middle panel in Figure 4. The right panel depicts the cloud digitization MISR results of the height of the clouds around 54°N (as denoted by the black arrows). It indicates that most of the cloud heights are below 2 km, which agrees with the MODIS heights. MISR cloud digitization of the heights of the cloud around 89°W and 48°N reveals high cloud heights (Figure 5) with values between 5 and 10 km, which again match the MODIS cloud heights. Therefore, MISR and MODIS agree with the cloud height values.

4.5 Analysis of cases under different cloud and pollution conditions

In this section, additional cases are investigated by analyzing the cloud filtered (standard) and the non-cloud masked, along with the MODIS cloud height and cloud mask products. Figure 6 shows the results over Canada, on 12 April 2010 and it indicates that, about 70% of the data are missing in the standard retrievals (Figure 6a). However, the non-cloud masked product (Figure 6b) captures notable features between 54°N–56°N and 90°W–98°W (as indicated by the red colors in Figure 6b). The MOPITT cloud flag description on 12 April 2010 (Figure 6d) reveals that all L2 data were retrieved under clear conditions (MODIS cloud percent less than 5%) as indicated by the flag number 2 (grey color) and the MOPITT diagnostics data (Figure 6c). However, the corresponding MODIS cloud height (Figure 6e) showed an area of very low cloud heights that are less than 500 m (around 54°N–56°N), where the MOPITT measurements were not retrieved completely in the standard product as they were considered cloudy (with more than 5% cloud cover, see Figure 6f). Comparing this area to the collocated non-masked CO product (Figure 6b), it can be noted that it exactly matches the coherent pattern that was observed between 54°N–56°N. Looking to IASI CO TC for the same time and location on 12 April 2010 (Figures 6c), it can be seen that most of the CO features in the area of 52-56 latitude and -100: -92 longitudes (Figure 6b) are not captured as well due to their cloud detection scheme.

An unusually active forest fire season occurred in the vicinity of Fort McMurray, Alberta, in May 2016. Three more cases at that time were examined. These are shown in Figures 7, 8, and 9. Figures 7a, 8a, and 9a and 7b, 8b, and 9b show the standard and non-standard CO TC on 6 (day), 16 (night), and 22 (day) May 2016, respectively. Again, the non-standard CO product on 6 and 16 May 2016 exhibits a notable coherent pattern over some areas that were not retrieved in the standard product. On 6 May 2016, there is a CO plume around 50°N–52°N and 108°W–112°W longitude that is indicated by the purple colors (Figure 7b) and it is completely missed in the standard product. On the other hand, IASI shows a consistency with the non-masked MOPITT

https://doi.org/10.5194/amt-2021-112
Preprint. Discussion started: 12 May 2021

Atmospheric Measurement Techniques Discussions

product where a prominent CO plumes was observed around 50-56 latitude and -112: -104 longitudes which coincide the corresponding MOPITT (Figure 7b)

On 16 May 2016, between 56°N–60°N and 118°W–120°W, a significant high CO feature is observed in the non-masked product (Figure 8b) which is likely to be a result of Fort McMurray fire emissions in northern Alberta (as indicated by MODIS fire images, not shown). Considering the low cloud detection during the Fort McMurray fires, the MODIS cloud height data of the corresponding MOPITT pixels on 6 May 2016 (Figure 7e) suggest that none of the low cloud (blue colors) pixels were retrieved in the standard product as it is implied by the MOPITT flag number (Figure 7d) (all values are 2).

Regarding the night case of 16 May 2016, the situation is much better where most of the low cloud pixels are retrieved, as illustrated in Figure 8d. However, there is still a small area of low clouds (between 56°N–58°N) (Figure 8e) that is not captured in the standard product, and is collocated with the missing biomass burning plume. However, on 16 May 2016, IASI (Figures 8c) could not capture the CO strong feature that are detected in MOPITT non-cloud-masked product (Figure 8b) around 56-58 latitude -120: -116 longitudes due to clouds, hence it matches the MOPITT CO standard one (Figure 8a).

In contrast to the above case studies, the non-masked CO observations on 22 May 2016 (Figure 9b) exhibited a different behavior. First, they did not reveal any strong coherent features similar to those that were shown in the previous examples. Second, although the cloud detection scheme was masked, the retrieval of some pixels was not successful, resulting in an area of missing data in the middle of the image (around 50°N–52°N). Comparing this area to the true image (not shown), these missing data were collocated with a comma shaped cloud. The MODIS cloud height values on 22 May 2016 (Figure 9e) over the comma region are more than 10 km which explains why the retrieval did not converge in the non-standard product. Thus, the retrieval algorithm is influenced by the cloud height and hence cloud height can play an important role in determining the retrieval quality. It is interesting to note that the comma shaped cloud (a specific cloud distribution pattern that is strongly associated with cyclone formulation) area separates an apparent higher CO amount to the west and lower amount to the east. In both these areas the clouds are low enough (<3 km) so that retrievals could be considered valid.

https://doi.org/10.5194/amt-2021-112
Preprint. Discussion started: 12 May 2021

Atmospheric Measurement Techniques Discussions

4.6 Global assessment of the potential use of MODIS cloud height

The case studies above indicate that if the low cloud areas were included in a future MOPITT retrieval scheme, there would be an increase of successful MOPITT retrievals. To assess the impact of this change, cloud heights were averaged for each MOPITT pixel of the non-retrieved L1 data. We added the current retrieval count to the cloud heights for a given height level at each MOPITT pixel and dividing it by the total number of MOPITT observations (L1). In that case MOPITT observations would increase by 5% if we included heights of 0.5 km, 10% at 1 km, and 30% at 2 km. These increases are not overwhelming, but these features are extremely important because they often occur close to intense fire features and large CO emissions. However, quality indices would then be needed as using the low cloud issue as the only criterion could degrade the retrieval.

4.7 Quality index measure of cloud detection scheme

In order to find an index measure that is sensitive to the retrieval algorithm, several parameters were examined, such as the relative error, iteration number (number of iterations before retrieval converges), degrees of freedom and L2 MOPITT chi-square χ^2 for masked and non-masked products. It was found that the χ^2 parameter often correlates with changes in the cloud detection algorithm, so χ^2 was chosen for the cloud detection assessment. Figures 10a and 10b depict the MOPITT χ^2 for standard and non-standard products on 16 August 2018, respectively. They indicate that the average value of χ^2 is below 10 for clear regions (Figure 10b). Comparing χ^2 for the non-standard product with the corresponding MODIS cloud heights (Figure 3e), it can be seen that the average χ^2 is still below 10 where cloud heights are less than 2 km. However, the values increase to 100 for the pixels that have cloud heights greater than 4 km. Repeating the same analysis retrievals on 12 April 2010 (Figures 10c and 10d) and 6 May 2016 (Figures 10e and 10f) reveals two extreme χ^2 values, 10 and 100. The highest and the lowest values are collocated with high and low clouds, respectively, as can be seen by comparison with MODIS cloud heights (Figures 6e and 7e). Hence, a χ^2 threshold value (e.g. 10) could be a proxy for the cloud height limit that should be included in the retrieval, and can be used as an index measure in the cloud detection scheme.

5. Conclusion

In this study, an analysis has been performed to consider the issue of increasing the number of MOPITT observations. The current MOPITT L2 data has ~30% successful retrievals, and so any process that could improve this number would be welcome. Since MOPITT retrievals are only performed in clear conditions, different retrieval approaches in cloudy conditions were initially considered, such as that used by AIRS, TES, and TROPOMI. The schemes used for retrievals by TES and TROPOMI were not applicable due to the lack of spectral information and good methane data, respectively. In addition, the approach used by AIRS was not suitable because the results of reconstructed clear column radiances of adjacent pixels were not sufficiently stable and precise. As a result, the analysis here focused on improving the existing MOPITT cloud detection scheme. The standard (cloud filtered) CO TC (L2) product was compared with a non-standard (non-cloud masked) version of the retrievals for selected days. The results reveal some interesting structures that were observed frequently in the non-cloud masked product compared to the standard product. Those features are not captured in the standard product because the current cloud detection scheme does not properly detect many low cloud cases over land. Hence, it is recommended to find a method to incorporate MODIS cloud height to improve the low cloud detection issue. A global assessment of the potential inclusion of MODIS cloud height revealed that the coverage of the MOPITT CO dataset would increase when the low cloud heights are properly incorporated in the cloud detection scheme. However, quality confidence flags must be assigned for each retrieval to maintain retrieval quality. It was found that, the retrieval quality is sensitive the cloud height values and the χ^2 parameter could be used as a quality measure.

ACKNOWLEDGMENTS

The authors would like to thank the CSA (Canadian Space Agency) for their financial support of this research. NCAR (National Center for Atmospheric Research) is sponsored by the National Science Foundation and operated by the University Corporation for Atmospheric Research. The NCAR MOPITT project is supported by the National Aeronautics and Space Administration (NASA) Earth Observing System (EOS) Program. The MOPITT team acknowledges support from the Canadian Space Agency (CSA), the Natural Sciences and Engineering Research Council (NSERC) and Environment Canada, and the contributions of

COMDEV (the prime contractor) and ABB BOMEM. The authors thank the AERIS infrastructure (http://www.aeris-data.fr) for providing access to the IASI CO data.

6. References

Ackerman, S. A., K. I. Stabala, W. P. Menzel, R. A. Frey, C. Moeller, and L. E. Gumley (1998), Discriminating clear sky from clouds with MODIS, J. Geophys. Res., 103, 32,141 – 32,157, doi:10.1029/ 1998JD200032.

Ackerman, S. A., R. E. Holz, R. Frey, E. W. Eloranta, B. Maddux, and M. J. McGill (2008), Cloud detection with MODIS: Part II. Validation, J. Atmos. Oceanic Technol., 25, 1073 – 1086.

Buchholz, R. R., M. N. Deeter, H. M. Worden, J. Gille, D. P. Edwards, J. W. Hannigan, N. B. Jones, C. Paton-Walsh, D. W. T. Griffith, D. Smale, J. Robinson, K. Strong, S. Conway, R. Sussmann, F. Hase, T. Blumenstock, E. Mahieu, and B. Langerock (2017), Validation of MOPITT carbon monoxide using ground-based Fourier transform infrared spectrometer data from NDACC, *Atmos. Meas. Tech.*, *10*(5), 1927–1956, doi:10.5194/amt-10-1927-2017.

Buchholz, R. R., Worden, H. M., Park, M., et al., Air pollution trends measured from Terra: CO and AOD over industrial, fire-prone, and background regions, Remote Sensing of Environment, 256, 112275, doi: 10.1016/j.rse.2020.112275, 2021.

Clerbaux, C., Boynard, A., Clarisse, L., George, M., Hadji-Lazaro, J., Herbin, H., ... & Coheur, P. F. (2009). Monitoring of atmospheric composition using the thermal infrared IASI/MetOp sounder. *Atmospheric Chemistry and Physics*, *9*(16), 6041-6054.

Deeter, M. N., Edwards, D. P., Francis, G. L., Gille, J. C., Martínez-Alonso, S., Worden, H. M., & Sweeney, C. (2017). A climate-scale satellite record for carbon monoxide: the MOPITT Version 7 product.

Deeter, M. N., Emmons, L. K., Francis, G. L., Edwards, D. P., Gille, J. C., Warner, J. X., ... & Yudin, V. (2003). Operational carbon monoxide retrieval algorithm and selected results for the MOPITT instrument. *Journal of Geophysical Research: Atmospheres*, *108*(D14).

Deeter, M. N., Worden, H. M., Gille, J. C., Edwards, D. P., Mao, D., & Drummond, J. R. (2011). MOPITT multispectral CO retrievals: Origins and effects of geophysical radiance errors. *Journal of Geophysical Research: Atmospheres*, *116*(D15).

Drummond, J. R., & Mand, G. S. (1996). The Measurements of Pollution in the Troposphere (MOPITT) instrument: Overall performance and calibration requirements. *Journal of Atmospheric and Oceanic Technology*, *13*(2), 314-320.

Drummond, J. R., Zou, J., Nichitiu, F., Kar, J., Deschambaut, R., & Hackett, J. (2010). A review of 9-year performance and operation of the MOPITT instrument. *Advances in Space Research*, *45*(6), 760-774.

Duncan, B. N., Logan, J. A., Bey, I., Megretskaia, I. A., Yantosca, R. M., Novelli, P. C., ... & Rinsland, C. P. (2007). Global budget of CO, 1988–1997: Source estimates and validation with a global model. *Journal of Geophysical Research: Atmospheres*, *112*(D22).

Edwards, D. P., Emmons, L. K., Gille, J. C., Chu, A., Attié, J. L., Giglio, L., ... & Ziskin, D. C. (2006). Satellite-observed pollution from Southern Hemisphere biomass burning. *Journal of Geophysical Research: Atmospheres*, *111*(D14).

Jiang, Z., Jones, D. B., Kopacz, M., Liu, J., Henze, D. K., & Heald, C. (2011). Quantifying the impact of model errors on top-down estimates of carbon monoxide emissions using satellite observations. *Journal of Geophysical Research: Atmospheres*, *116*(D15).

Kulawik, S. S., J. Worden, A. Eldering, K. Bowman, M. Gunson, G. B. Osterman, L. Zhang, S. Clough, M. W. Shephard, and R. Beer (2006), Implementation of cloud retrievals for Tropospheric Emission Spectrometer (TES) atmospheric retrievals: part 1. Description and characterization of errors on trace gas retrievals, J. Geophys. Res., 111, D24204, doi:10.1029/2005JD006733.

Landgraf, J., aan de Brugh, J., Scheepmaker, R., Borsdorff, T., Hu, H., Houweling, S., Butz, A., Aben, I., and Hasekamp, O.: Carbon monoxide total column retrievals from TROPOMI shortwave infrared measurements, Atmos. Meas. Tech., 9, 4955–4975, https://doi.org/10.5194/amt-9-4955-2016, 2016.

Li, J., Liu, C. Y., Huang, H. L., Schmit, T. J., Wu, X., Menzel, W. P., & Gurka, J. J. (2005). Optimal cloud-clearing for AIRS radiances using MODIS. *IEEE Transactions on Geoscience and Remote Sensing*, *43*(6), 1266-1278.

https://doi.org/10.5194/amt-2021-112
Preprint. Discussion started: 12 May 2021

Marey H., Drummond J., (2018). Analysis of MOPITT Cloud-Clearing Algorithm V3-V7. Internal report for “MOPITT Data Enhancements through Improved Cloud Clearing “project.

Moeller, C. and Frey, R.: Terra MODIS Collection 6.1 Calibration and Cloud Product Changes, Version 1.0, available at: https://modis-atmosphere.gsfc.nasa.gov/sites/default/files/ModAtmo/C6.1_Calibration_and_Cloud_Product_Changes_UW_frey_CCM_1.pdf (last access: 16 March 2021), 2017.

Nelson, D. L., Garay, M. J., Kahn, R. A., & Dunst, B. A. (2013). Stereoscopic height and wind retrievals for aerosol plumes with the MISR INteractive eXplorer (MINX). *Remote Sensing*, *5*(9), 4593-4628.

Nelson, D., Khan R., Tosca M., Val S., and M. Garay, C. (2015), MISR Interactive eXplorer (MINX) V4 user’s guide, report, Jet Propuls. Lab., Pasadena, Calif. (Available at https://github.com/nasa/MINX/blob/master/webdoc/MINX_HowToDigitize.pdf).

Spivakovsky, C. M., Logan, J. A., Montzka, S. A., Balkanski, Y. J., Foreman-Fowler, M., Jones, D. B. A., ... & Wofsy, S. C. (2000). Three-dimensional climatological distribution of tropospheric OH: Update and evaluation. *Journal of Geophysical Research: Atmospheres*, *105*(D7), 8931-8980.

Strode, S. A., & Pawson, S. (2013). Detection of carbon monoxide trends in the presence of interannual variability. *Journal of Geophysical Research: Atmospheres*, *118*(21), 12-257.

Susskind, J., Barnet, C. D., & Blaisdell, J. M. (2003). Retrieval of atmospheric and surface parameters from AIRS/AMSU/HSB data in the presence of clouds. *IEEE Transactions on Geoscience and Remote Sensing*, *41*(2), 390-409.

Vidot, J., Landgraf, J., Hasekamp, O. P., Butz, A., Galli, A., Tol, P., & Aben, I. (2012). Carbon monoxide from shortwave infrared reflectance measurements: A new retrieval approach for clear sky and partially cloudy atmospheres. Remote sensing of environment, 120, 255-266.

Warner, J. X., Gille, J. C., Edwards, D. P., Ziskin, D. C., Smith, M. W., Bailey, P. L., & Rokke, L. (2001). Cloud detection and clearing for the Earth Observing System Terra satellite Measurements of Pollution in the Troposphere (MOPITT) experiment. *Applied Optics*, *40*(8), 1269-1284.

https://doi.org/10.5194/amt-2021-112
Preprint. Discussion started: 12 May 2021

Atmospheric Measurement Techniques
Discussions

473 Worden, H. M., Deeter, M. N., Frankenberg, C., George, M., Nichitiu, F., Worden, J., ... & De Laat, A. T. J. (2013). Decadal record of satellite carbon monoxide observations. *Atmospheric Chemistry and Physics*, *13*(2), 837-850.

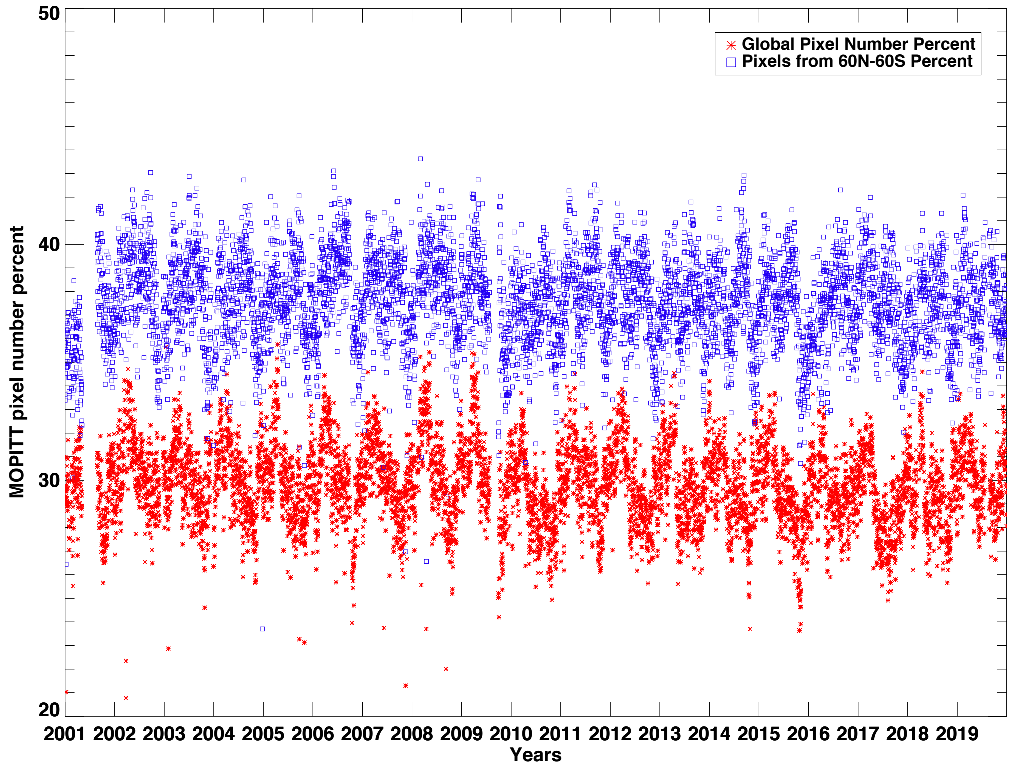

Figure (1) The percentage of successful daily MOPITT retrievals between 90°S–90°N and 60°S–60°N from 2000 to 2019.

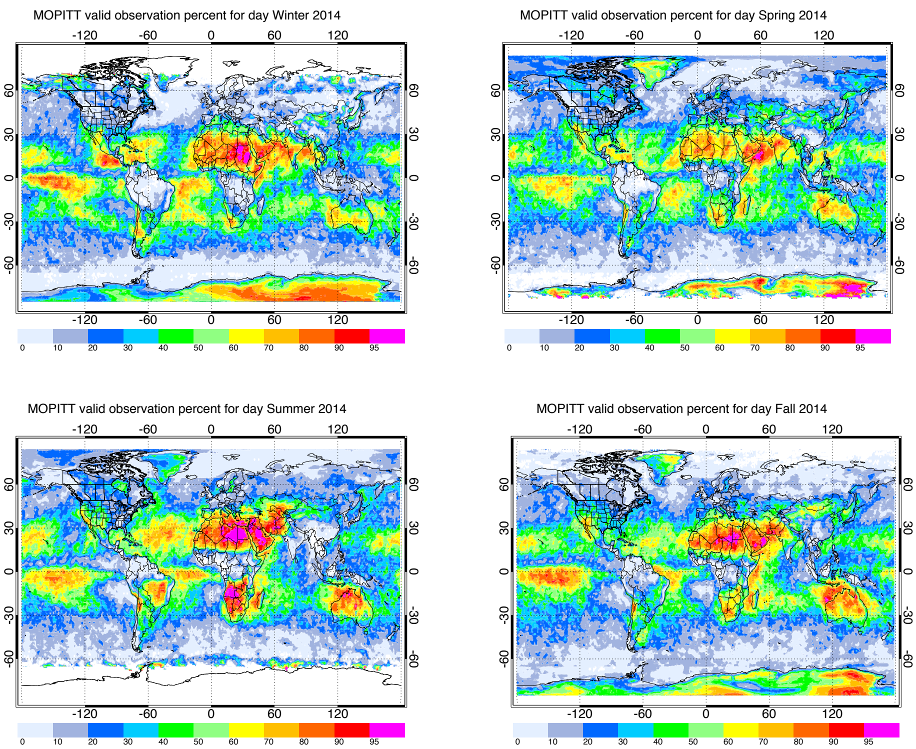

Figure (2) Seasonally averaged spatial distribution of the valid MOPITT retrievals in 2014. Data were aggregated into 1° × 1° bins.

https://doi.org/10.5194/amt-2021-112
Preprint. Discussion started: 12 May 2021

Atmospheric Measurement Techniques
Open Access
Discussions

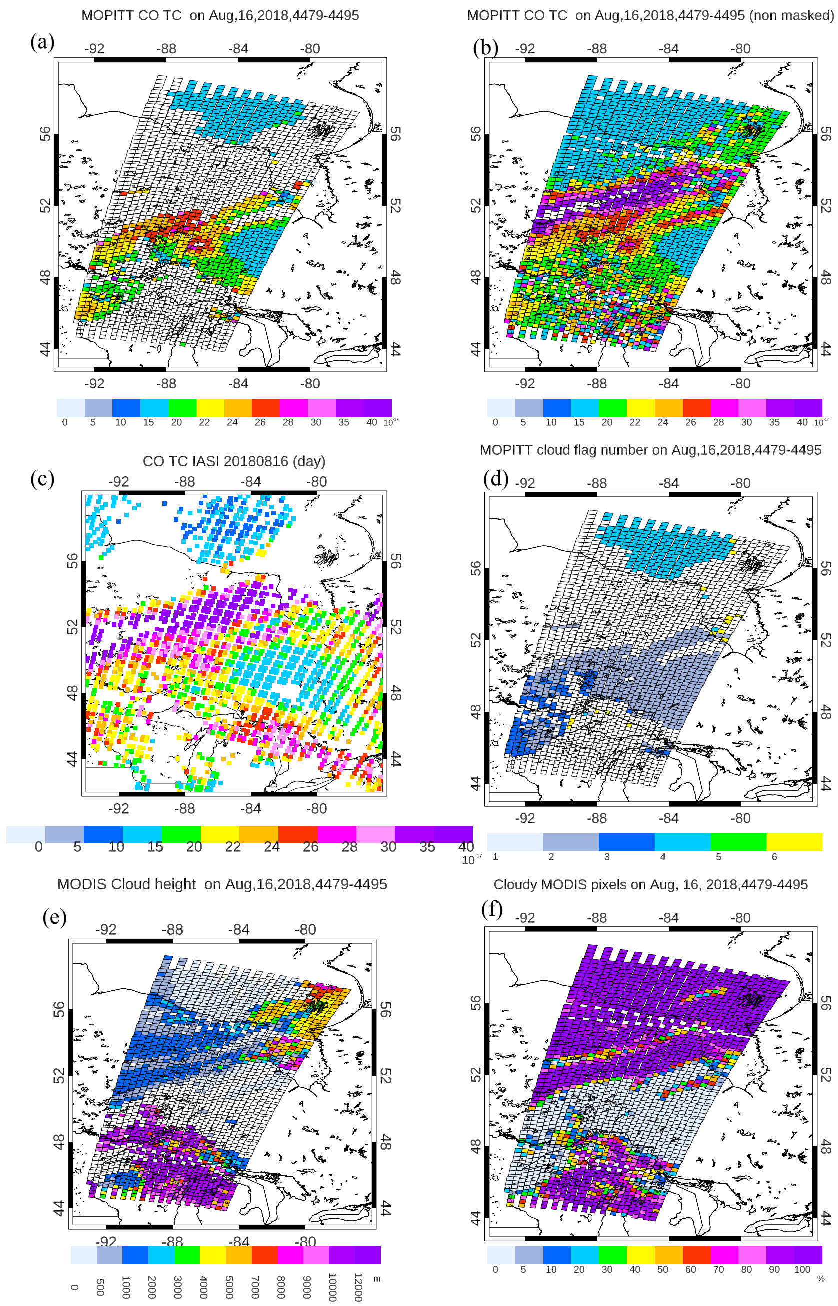

Figure 3. (a) Standard (cloud masked), (b) non-standard (non-cloud masked) CO TC, (c) IASI CO TC, (d) flag number, (e) MODIS cloud height, and (f) cloud mask on 16 August, 2018. The faint black squares represent MOPITT pixels (22 km x 22 km) for all L1 observations.

https://doi.org/10.5194/amt-2021-112
Preprint. Discussion started: 12 May 2021

Atmospheric Measurement Techniques
Discussions

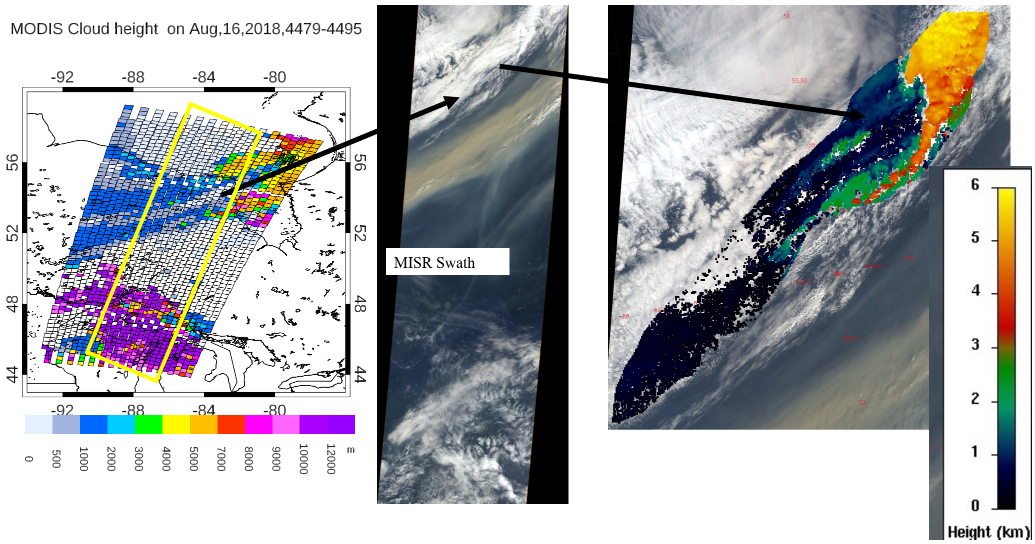

Figure (4) MODIS cloud height (left panel), MISR swath (middle panel), and cloud digitization of the height of the clouds around 54°N using MISR data (right panel) on 16 August 2018.

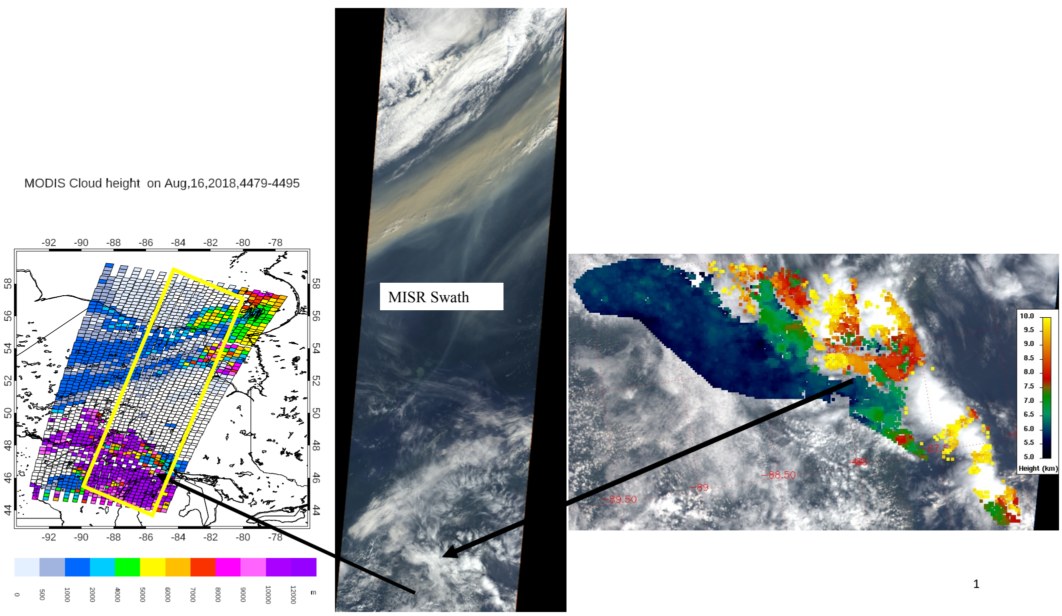

Figure (5) MODIS cloud height (left panel), MISR swath (middle panel), and cloud digitization of the height of the clouds around 89°W and 48°N using MISR data (right panel) on 16 August 2018.

https://doi.org/10.5194/amt-2021-112
Preprint. Discussion started: 12 May 2021

Atmospheric Measurement Techniques
Discussions

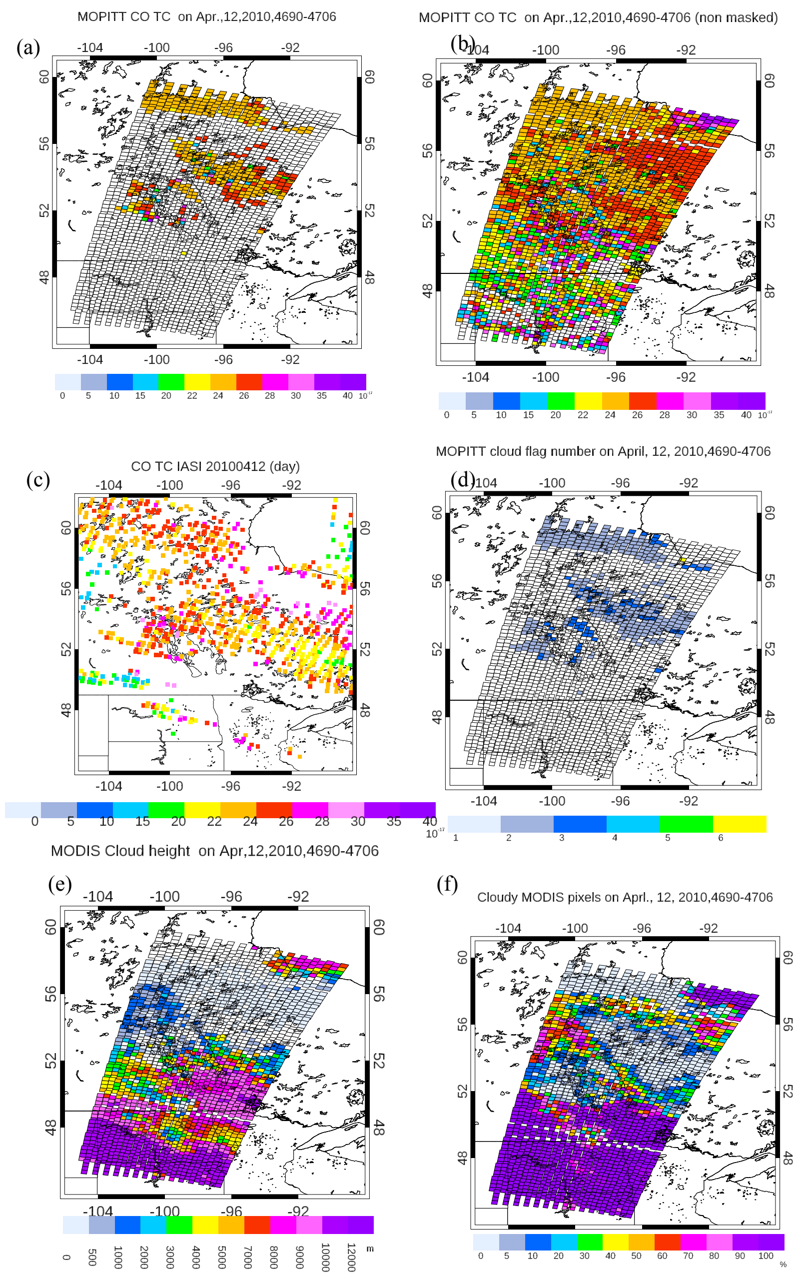

Figure (6) The same as Figure 3, but for 12 April 2010.

https://doi.org/10.5194/amt-2021-112
Preprint. Discussion started: 12 May 2021

Atmospheric Measurement Techniques
Discussions

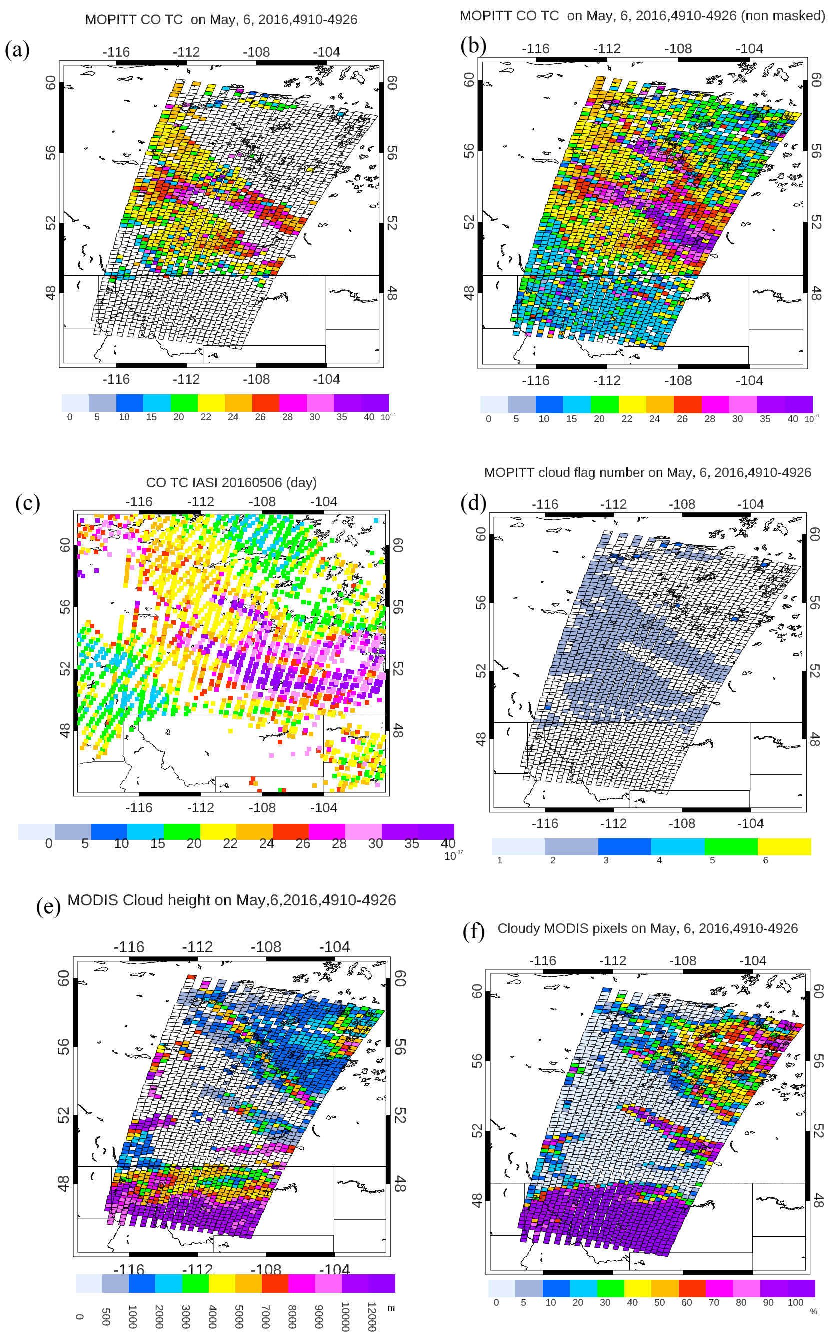

Figure (7) The same as Figure 3, but for 6 May 2016.

https://doi.org/10.5194/amt-2021-112
Preprint. Discussion started: 12 May 2021

Atmospheric Measurement Techniques
Open Access
Discussions

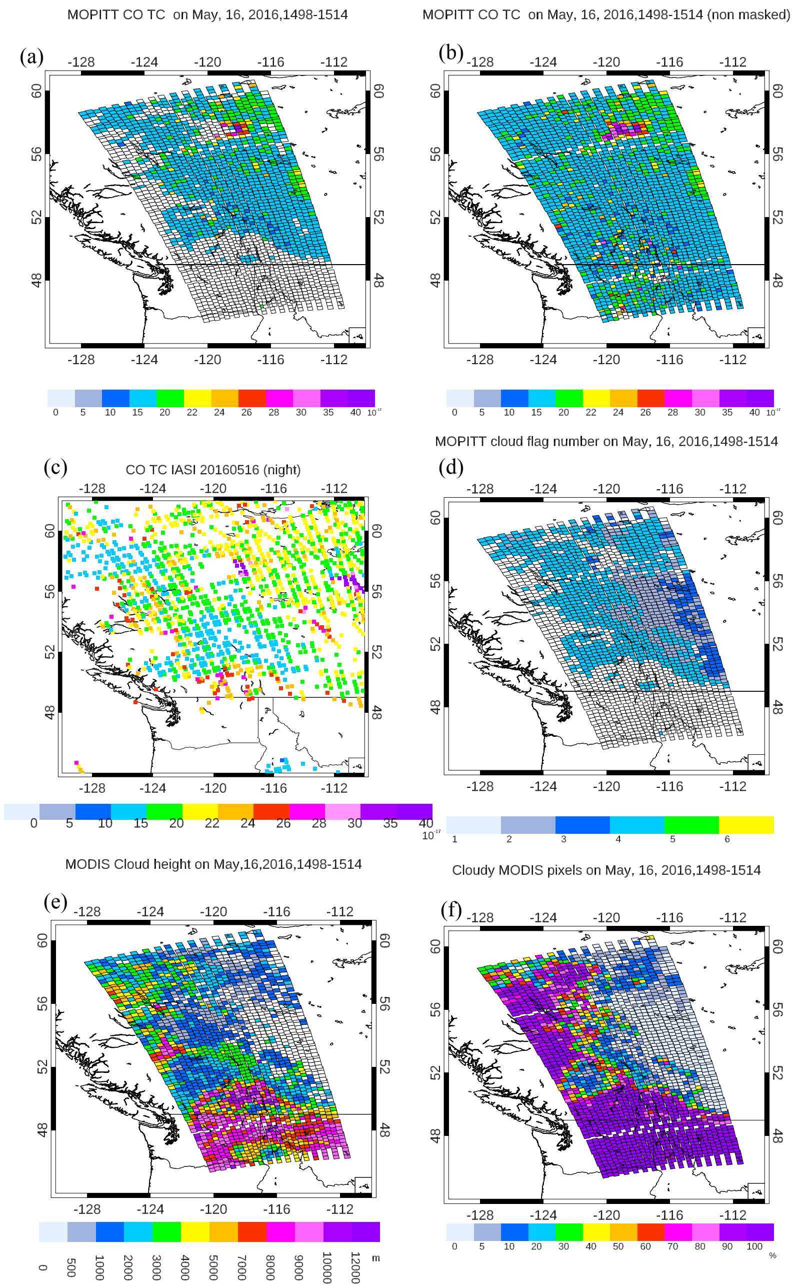

Figure (8) The same as Figure 3, but for 16 May 2016.

Atmospheric Measurement Techniques Discussions

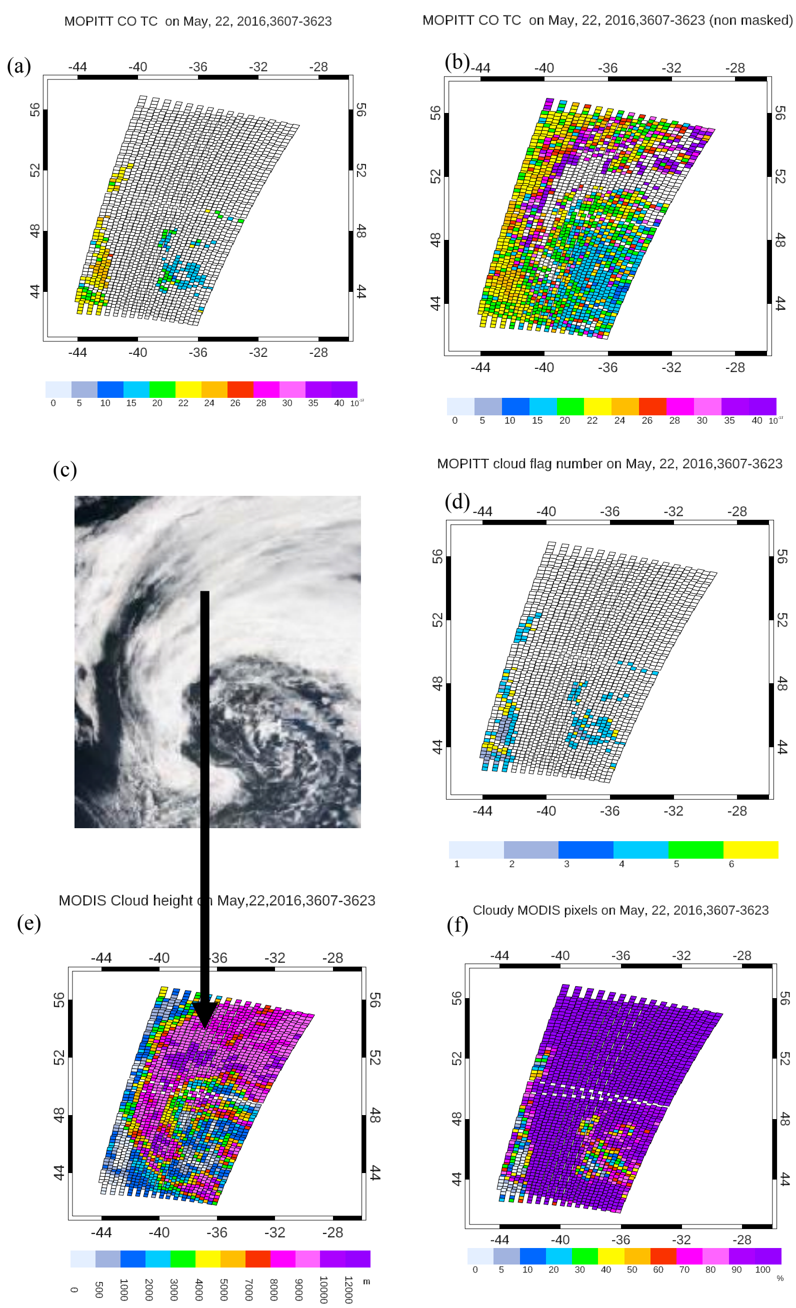

Figure (9) The same as Figure 3, but for 22 May 2016.

https://doi.org/10.5194/amt-2021-112
Preprint. Discussion started: 12 May 2021

Atmospheric Measurement Techniques
Discussions

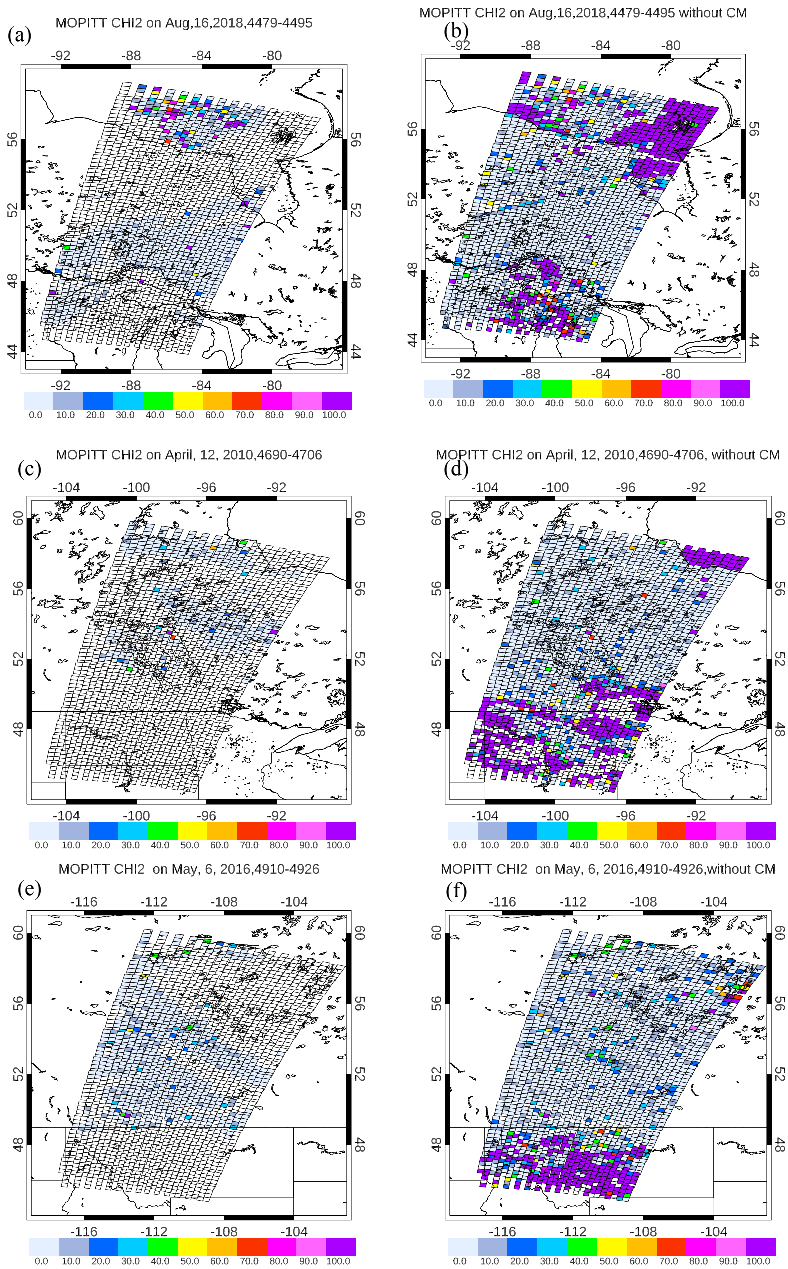

Figure (10) χ^2 for the standard product on (a) 16 August 2018, (c) 12 April 2010, and (e) 6 May 2016, and for the non-standard product on (b) 16 August 2018, (d) 12 April 2010, and (f) 6 May 2016.